Induction of the aggresome and insoluble tau aggregation using an optogenetic tool

Shigeo Sakuragi[1], Tomoya Uchida[1#], Naoki Kato[1#], Boxiao Zhao[1], Akito Hattori[1$], Yoshihiro Sakata[1], Yoshiyuki Soeda[2], Akihiko Takashima[2], Hideaki Yoshimura[3], Gen Matsumoto[4], Hiroko Bannai[1*]

[1] *Department of Electrical Engineering and Biosciences, School of Advanced Science and Engineering, Waseda University, Shinjuku-Ku, Tokyo 162-0056, Japan.*

[2] *Laboratory for Alzheimer's Disease, Department of Life Science, Faculty of Science, Gakushuin University, Toshima-ku, Tokyo 171-8588, Japan*

[3] *Department of Chemistry, School of Science, The University of Tokyo, Tokyo 113-0033, Japan*

[4] *Department of Neurological Disease Control, Graduate School of Medicine, Osaka Metropolitan University, Osaka, 545-8585, Japan*

 # Equally contributed

$ Current affiliation： Department of Medical Laboratory Science, Kitasato University School of Health Sciences, Minami-Uonuma, 949-7241, Japan

Corresponding author: Hiroko Bannai, School of Advanced Science and Engineering, Department of Electrical Engineering and Biosciences, Waseda University, 2-2 Wakamatsu-cho, Shinjuku-Ku, Tokyo 162-0056, Japan. ORCID iD: https://orcid.org/0000-0002-0951-488X e-mail: hiroko.bannai@waseda.jp

ABSTRACT

Tauopathy is a group of diseases where fibrillary tau aggregates are formed in neurons and glial cells in the brain. In Alzheimer's disease (AD), the most common form of tauopathy, tau aggregation begins in the brainstem and entorhinal cortex and then spreads throughout the brain. Understanding the mechanism by which locally formed tau pathology propagates throughout the brain is crucial for comprehending the pathogenesis of AD. Therefore, a novel model of tau pathology that artificially induces tau aggregation in targeted cells at specific times is essential. In this study, we report a novel optogenetic module, OptoTau, human tau with the P301L mutation fused with a photosensitive protein CRY2Olig, which could induce various forms of tau depending on the pattern of blue light illumination. Continuous blue light illumination for 12 h to Neuro2a cells stably expressing OptoTau (OptoTauKI cells) resulted in cluster formation along microtubules, many of which eventually accumulated in aggresomes.

On the other hand, when alternating light exposure and darkness in 30-minute cycles for 8 sets per day were repeated over 8 days, methanol-insoluble tau aggregation was formed. Methanol-insoluble tau was induced more rapidly by repeating cycles of 5-minute illumination followed by 25 minutes of darkness over 24 hours. These findings suggest that OptoTau can induce various stages of tau aggregation depending on the pattern of blue light exposure. Thus, this technique holds promise as a novel approach to creating specific tau aggregation in targeted cells at desired time points.

Keywords: Tauopathy, Alzheimer's disease, CRY2Olig

Significance

In this study, we established a technique to manipulate tau aggregation in a blue light-dependent manner using cells stably expressing OptoTau, an optogenetic tool based on the CRY2Olig module. Tau accumulation in aggresomes or insoluble tau aggregation were specifically induced in response to blue light illumination conditions. These results are significant in that they provide a new technological basis for creating a singular point of tau aggregation in specific targeted cells at a targeted time.

Introduction

Tauopathy is a group of diseases in which neurofibrillary tangles (NFTs), filamentous tau protein aggregates, are formed in neurons and glial cells in the brain[1]. Despite being triggered by abnormalities in the same molecule tau, tauopathy manifests as various disorders such as Alzheimer's disease (AD), Pick's disease, progressive supranuclear palsy (PSP), corticobasal degeneration (CBD), chronic traumatic encephalopathy (CTE). In healthy neurons, microtubule-binding protein tau plays physiological roles, such as neurite outgrowth and regulation of axonal transport by motor proteins. However, tau detaches from microtubules and forms intracellular tau aggregates when tau is subject to post-transcriptional modifications such as excessive phosphorylation [2]. In AD, the most common form of tauopathy, the hyperphosphorylation of tau as a cause of NFT is initially formed in the neurons in locus coeruleus (LC) and entorhinal cortex (EC) [3] [4]. This tau aggregation expands with age into the transentorhinal region, hippocampus, and cerebral cortex (temporal lobe, prefrontal cortex, and higher sensory association neocortex) [4]. The progression of tau aggregation is closely associated with the development of clinical pathology of AD [5] [6].

Several model experimental systems have contributed to understanding the relationship between the accumulation of degenerative tau and higher brain functions in AD and the mechanisms underlying the expansion of tau pathology. In mice overexpressing neurons with human tau with the mutation in 301st proline to serine or leucine (P301S or P301L) found in familial frontotemporal dementia, tau aggregate formation, synapse loss, neurodegeneration, and brain atrophy have been observed in a few months [7] [8] [9] [10]. Because these phenotypes have much in common with the pathology in human patients, these mice have served as a model for AD, contributing to the elucidation of the mechanism of toxicity from degenerated tau. Tau filaments polymerized in vitro and insoluble tau fractions from AD patients injected into human tau-overexpressing mice form hyperphosphorylated tau and tau aggregates in distant brain regions with neuronal connections [11] [12] [13]. Tau extracted from patient brains also induces pathology, even in non-transgenic mice [14] [15]. The spread of degenerated tau to healthy neurons has been shown to occur through synaptic contact or by uptake by other cells of degenerated tau released extracellularly in a synaptic activity-dependent manner [16] [17]. These experiments have contributed to elucidating some aspects of the pathogenesis of tauopathy as model systems that rationally reproduce some of the phenotypes seen in Alzheimer's disease and other tauopathies in humans.

Recently, Nagai et al. defined a "singularity phenomenon" as a biological phenomenon in which a small number of rare cells cause significant changes throughout a complex system, and these small number of rare cells are

named "singularity cells" [18] [19]. From this perspective, neurons that first accumulate hyperphosphorylated tau and NFTs in LCs and ECs can be regarded as "singularity cells" in AD [20]. How do these "singularity cells" that initially accumulate tau arise? How is the degeneration of tau transmitted from the singularity cells to the entire cortex? Addressing these questions is considered crucial for understanding the onset mechanisms of AD. However, to address this issue, the current experimental system of tauopathy models has several challenges to overcome. Although regions in the brain tend to aggregate tau, identified in tauopathy model mice with human tau overexpression, it remains unclear when the first "singularity cells" that accumulate tau are born and why they can produce tau aggregation. More seriously, the loss of endogenous genes and uncertain protein expression levels of transduced tau in human Tau overexpression model animals have been found, and whether the phenotypes obtained so far are due to abnormalities in tau requires reconsideration [10]. Another AD model, obtained by injecting exogenous tau seeds, bypasses the initial process of AD pathogenesis, tau aggregation. Tau seed uptake is entirely random, and it is impossible to identify the cell from which the pathology originates. A new model system is needed to create a singular point of tau aggregation at a targeted time in specifically targeted cells to elucidate the process of tau pathology from the singularity cells, neurons that first develop tau pathology.

In this study, we applied optogenetics to induce tau aggregation in targeted cells. CRY2, a photoreceptor in *Arabidopsis*, and its derivative CRY2Olig are optogenetic modules that form oligomers reversibly upon exposure to blue light [21]. Recently, researchers have introduced CRY2 to induce aggregation of proteins found in neurodegenerative diseases, including tau [22] [23] [24] [25]. CRY2 and tau fusion proteins accumulated on microtubules by liquid-liquid phase separation (LLPS) induced by blue light illumination [23]. Blue light illumination forms tau droplets and oligomers in primary cortical culture neurons of mice overexpressing tau fused with CRY2Olig, a higher capacity for homo-oligomer formation [24]. We have recently shown that 'OptoTau,' a fusion of human tau with the P301L mutation and CRY2Olig, transiently overexpressed in Neuo2a cells, could induce LLPS droplets and oligomers of tau by illuminating blue light for 24 hours [25]. In the present study, we manipulated intracellular tau by blue light illumination in Neuro2a cells stably expressing OptoTau. OptoTau, inserted into the safe-harbor region by CRISR/Cas9 technique, was subjected to various temporal patterns of blue light illumination, including eight-day illumination. Here, we report that different patterns of blue light illumination allow the same optogenetic tool, OptoTau, to induce opposite responses: induction of tau degradation by aggresome and formation of insoluble tau aggregates.

Materials and Methods

OptoTau knock-in into Neuro2a cells

OptoTau consists of the optogenetic module CRY2olig [21], a SNAP-tag, and a full-length human tau (2N4R) with a P301L (Figure 1A). OptoTau-donor vector, OptoTau gene under the CMV promoter, and GFP and Puromycin resistant genes under the EF1α promoter were constructed using ROSA26 MCS. The OptoTau-donor vector and mROSA26sgRNA/Cas9 vector (GeneCopoeia), including the guide RNA and Cas9 sequences, were transfected into mouse neuroblastoma-derived Neuro2a cells (JCRB Cell Bank) using Lipofectamine 3000 (Life Technologies). Drug selection was performed by adding 400 μg/ml G418 (Nacalai tesque) on day one post-transfection and 1 μg/ml puromycin (Nacalai tesque) 4 days later. GFP was used as a marker for gene insertion, and GFP-positive cells were isolated into a 96-well plate. Single colonies of GFP-positive cells were replated into a 24-well plate and further expanded on a 10 cm culture dish. After confirming the expression of OptoTau, one clone was used as OptoTau Knock-in (OptoTauKI) cells in this study.

Cell Maintenance

OptoTauKI and Neuro2a wild type (WT) were maintained in Dulbecco's Modified Eagle's medium (4.5 g/l glucose; Nacalai tesque) supplemented with 10% FBS, penicillin (100 units/ml) streptomycin (100 μg/ml) mixture, in 5% CO_2, 37°C environment. OptoTauKI cells were kept under light-shielded conditions to prevent irregular CRY2olig conformational changes caused by room light. For the live imaging experiment, cells were plated on a 35 mm glass bottom dish (MATSUNAMI) coated with 0.04% Polyethyleneimine (PEI, Sigma-Aldrich). Cells were plated on an 18 mm cover glass precoated with 0.04% PEI for fixation. The density of light-exposed cells was always maintained at 60-80% confluence, except in the experiment where the cells were incubated for 48-72 hours after light illumination.

Blue light illumination

A blue light illumination device (TH2-211X200BL, CCS Inc.) was set in a 5% CO_2 incubator at 37°C. Plates of cells were placed on a transparent plastic box with a height of 30 mm on the light-emitting device. The light intensity was 0.24 ± 0.04 mW/cm^2 throughout all experiments. The illumination protocol, one 12-hour illumination, 8 cycles of 30-minute (min) illumination - 30-min light off per day for up to 8 days, and 48 cycles of 5-min illumination - 25-min light off per day, was performed in this study. An automatic timer controlled the illumination timing.

115

116 **Labeling of OptoTau using SNAP-tag**

117 Fluorescent labeling of OptoTau molecules was performed by covalently binding a fluorescent-labeled SNAP ligand to
118 a SNAP-tag inserted into the OptoTau. 0.1 μM SNAP-Cell 647-SiR (New England BioLabs) was administered into the
119 culture medium, and OptoTau KI or WT was applied for 12 to 18 hours. Cells were washed with medium and then used
120 for live cell imaging or immunocytochemistry.

121

122 **Immunocytochemistry**

123 Phosphate buffered saline (PBS) was used for dilution and washing throughout the immunocytochemistry. Cells were
124 generally fixed with 4% fixation in 4% paraformaldehyde (PFA) for 15 min at room temperature (RT) and
125 permeabilized with 0.1% Triton X-100 for 3 min at RT. For immunostaining of microtubule or aggresomal markers,
126 cells were fixed with ice-cold Acetone/Methanol (Acetone: Methanol =1:1) for 3 minutes at -20°C, followed by post-
127 fixation with 4% PFA (15 min, RT). To visualize insoluble tau, cells were fixed with ice-cold methanol for 20 min at -
128 20°C. This treatment removes soluble tau in the cytosol [26]. After fixation and permeabilization, cells were incubated
129 with 5% Bovine Serum Albumin (BSA) for 30 min RT for blocking, then with primary antibody treatment in 2.5%
130 BSA for 1 hour at RT. Primary antibodies used were: anti-total tau antibody (RTM38, 1:1000, Fujifilm), antibody
131 recognizing the initial structural change of pathological tau (MC1, 1:1000; gifted from Prof. Peter Davies [Albert
132 Einstein College of Medicine Medicine], anti-αTubulin antibody (1:2000; Sigma-Aldrich), anti-γTubulin antibody
133 (1:100; Santa Cruz), anti-HDAC6 antibody (1:100; Santa Cruz), anti-Dynein antibody (1: 100; Santa Cruz). After
134 washing with PBS, cells were incubated with secondary antibodies (5 μg/ml in 2.5% BSA) for 40 min, RT. Secondary
135 antibodies used were: Anti-rat IgG (H+L) Alexa Fluor® 555 conjugate, Anti-rat IgG (H+L) Alexa Fluor® 647
136 conjugate (Cell signaling) or Goat anti-Rat IgG (H+L) Cross-Adsorbed Secondary Antibody, Alexa Fluor™ 594, Goat
137 anti-Mouse IgG (H+L) Cross-Adsorbed Secondary Antibody, Alexa Fluor™ 647, Goat anti- Mouse IgG (H+L) Cross-
138 Adsorbed Secondary Antibody, Alexa Fluor™ 555 (Thermo Fisher Scientific).

139

140 **Observation by epifluorescence microscopy and confocal laser scanning microscopy**

141 Immunocytochemically or SNAP-tagged cells were observed using an inverted microscope (IX73; Evident) equipped
142 with a high-intensity LED driver (DC4104, Thorlabs) and a digital CMOS camera (ORCA-Fish 4.0; HAMAMATSU).
143 60x oil immersion objective (NA 1.42; Evident), and the optical zoom was set to 5x. 5-10 fields of view were captured

144 from a single cover glass. Confocal laser scanning microscope (FV3000; Evident) images were taken with an oil
145 immersion objective (×60, NA1.42; Evident) at 5x digital zoom.
146
147 **Image Analysis**
148 Epifluorescence or confocal microscopy images were contrast-adjusted using MetaMorph (Molecular Devices) or
149 ImageJ (NIH) image analysis software. The percentage of cells with insoluble tau aggregates in the field of view was
150 calculated per images of PFA-fixed samples. The presence of the aggregates was defined when the maximum RTM38
151 intensity value in the cell was larger than "the mean of the RTM38 intensity + 3 standard deviation" of the dark
152 condition. The presence of aggregates around the nucleus was measured at the focal plane, where the nucleus was
153 maximally visible and calculated as a percentage per coverslip.
154
155 **Western blotting**
156 Immediately after completion of blue light illumination, 2.0 x 10^6 cells/mL of WT Neuro2a or OptoTau KI cells were
157 incubated in 10 mM HEPES buffer supplemented with 1% protease inhibitor (cOmplete, Roche), 1 μM okadaic acid
158 (Cayman Chemical), 1 mM sodium orthovanadate (MP Biomedicals), 1 mM sodium fluoride (Nacalai tesque), 1 mM β-
159 glycerophosphate disodium salt hydrate (Sigma-Aldrich), 250 mM Sucrose, 1 mM EDTA. Samples were subjected to
160 15 s- sonication followed by 15 s- ice-cooling 4 times and centrifuged at 3000 x g for 10 min at 4°C. The supernatant
161 was mixed with non-reducing Tris-Glycine SDS sample buffer (06-363No, TEFCO) and was loaded onto a 5-20%
162 gradient gel. Samples were electrophoresed at 40 mA and transferred to a PVDF membrane (170-4156, Bio-Rad). After
163 transfer, the membrane was blocked with 1% BSA with 0.05% Tween-20 and reacted with an anti-tau antibody
164 (RTM38, 1:2500) and anti-β-actin antibody (1:10,000; A5441, Sigma-Aldrich) at 1h RT (or 4°C O/N). After washing
165 three times with PBST (0.05% Tween20 in PBS), the membrane was incubated with the secondary antibodies
166 conjugated with peroxidase (1:10,000, Jackson Immuno Research) at RT for 1h. Chemiluminescence signals were
167 detected using a luminol-based chemiluminescence assay kit (Chemi-Lumi One L, Nacalai tesque) and
168 chemiluminescence detection system (ChemiDoc Touch MP imaging system, Bio-Rad).
169
170 **Statistics**
171 Numbers of data are listed in Figure legends. The Mann-Whitney U test was used to compare Western blots with and
172 without blue light illumination and the percentage of cells with insoluble tau aggregates. Student's t-test was used to

173 compare the percentage of tau aggregates in the perinuclear region for each light exposure pattern. The p-values in each
174 figure are as follows: NS: $p > 0.1$, *: $p < 0.05$, ***:$p < 0.001$, ****:$p < 0.0001$.
175
176 **Results**
177
178 **Establishment of OptoTau knock-in (OptoTauKI) cells**
179 OptoTau is a protein fused to CRY2Olig [21], which forms multimeric complexes when exposed to blue light, with
180 human 2N4R tau carrying the P301L mutation (Figure 1A). We have previously shown that transient overexpression of
181 OptoTau into Neuro2a and exposure to blue light can induce the clustering of tau [25]. In this study, we established
182 Neuro2a cells stably expressing OptoTau and investigated the effects of blue light illumination over a longer period
183 than in previous studies. OptoTau was introduced into the mouse Safe Harbor ROSA26 region using the CRISPR/Cas9
184 system. We designed the cells to express OptoTau under the CMV promoter and GFP for screening under the EF1α
185 promoter (Figure 1A). We isolated GFP-positive single colonies and defined them as OptoTau Knock-in (OptoTauKI)
186 cells. To confirm the expression and localization of OptoTau, we performed fluorescent labeling of SNAP-tag
187 incorporated into OptoTau. No signal was observed in non-genome-edited Neuro2a cells (WT) for both GFP and
188 SNAP647 labeling, whereas in OptoTauKI cells, GFP was observed throughout the cells, and SNAP-tag signal was
189 observed in the cytoplasm (Figure 1B). Live cell imaging with a confocal microscope revealed that OptoTau was
190 localized in the cytoplasm, avoiding the nucleus (Figure 1C). These results indicate that OptoTau is inserted in
191 OptoTauKI cells and that the expressed OptoTau resides mainly in the cytoplasm.
192
193 **Formation of filament-like clusters of tau by 12-hour- blue light exposure**
194 Next, we examined the behavior of OptoTau in OptoTauKI cells under blue light illumination. OptoTauKI cells
195 were continuously exposed to blue light for 12 hours using a blue LED in a CO_2 incubator, then tau localization by
196 SNAP staining or immunofluorescence staining. In OptoTauKI cells cultured in the dark, both the SNAP signal and the
197 signal of total tau visualized by the RTM38 antibody showed uniform distribution in the cytoplasm (Figure. 2A, Dark).
198 In contrast, in OptoTau cells exposed to blue light for 12 hours, OptoTau labeled with SNAP647 formed thick filament-
199 like structures, also recognized by RTM38 antibody (Figure. 2A, 12 h blue light).
200 Single-molecule localization microscopy has shown that tau forms oligomers on microtubules [27]. To determine
201 whether the filamentous tau formed by blue light illumination co-localizes with microtubules, we performed multicolor

202 immunofluorescence staining of tau and microtubules in the same cells. OptoTauKI cells illuminated with blue light for
203 12 hours were fixed with acetone methanol, and microtubules were labeled with α-tubulin antibody and tau with
204 RTM38 antibody (Figure. 2B). The signal of filamentous tau largely colocalized with that of α-tubulin (Figure. 2B,
205 Merge).

206 Furthermore, the expression level of tau in OptoTauKI cells was confirmed by Western blot using RTM38
207 antibody. Only a 115 kDa band was detected in Neuro2a cells (WT), while two bands of 115 kDa and 150 kDa were
208 detected in OptoTauKI cells (OptoTau) with or without blue light exposure. Based on the molecular weights, the 115
209 kDa band can be interpreted as the tau dimer and the 150 kDa band as the OptoTau, conjugation of CRY2olig, SNAP,
210 and tau. To examine whether the amount of OptoTau protein changes with or without blue light illumination, the
211 intensity of the 115 kDa and 150 kDa bands were quantified. Band intensities were normalized by β-actin, a loading
212 control, and calculated as "relative tau intensity" relative to the value of Neuro2a cells (WT). The relative tau intensity
213 of the 115 kDa band was not different between the cells with and without 12 hours of blue light exposure (Figure. 2D,
214 115 kDa), while the relative tau intensity of the 150 kDa band was higher in the blue light group in 5 out of the 6
215 samples. These results indicate that the amount of OptoTau protein in OptoTauKI cells was increased by 12-hour- blue
216 light illumination.

217

218 **Tau dynamics in OptoTauKI cells after the termination of blue light illumination**

219 Twelve hours of blue light irradiation induced filament-like structures in OptoTauKI cells (Fig. 2A, B). At the same
220 time, tau aggregates with large molecular weights, which could be oligomers, were not detected by Western Blot (Fig.
221 2C). To examine the stability of filamentous tau formed after 12 hours of blue light illumination, cells were fixed at 12,
222 24, 48, and 72 hours after termination of blue light. The subcellular localization of tau and microtubules was examined
223 by immunofluorescence staining (Fig. 3A). In OptoTauKI cells immediately after blue light termination, filament-like
224 tau co-localized with microtubules, and a strong signal was found in part of them (Fig. 3B, 0 h, arrowheads). Twenty-
225 four hours after the termination of blue light, a bright spot with dense tau was formed in the vicinity of the nucleus (Fig.
226 3B, 24 h, arrowheads). Bright spots were still present at 48 and 72 hours, but the tau bright spot was fragmented in most
227 cells. These results suggest that the filamentous tau formed in OptoTauKI cells after 12 h of blue light illumination is
228 not a stable structure but an unstable one that can dynamically change morphology over time.

229

230 **Co-localization of tau with aggresome markers after blue light illumination**

231 Proteasome inhibition and uptake of tau-paired helical protofilaments from AD patients have been shown to induce
232 aggresomes, inclusion bodies for misfolded proteins [28] [29]. Aggresomes are formed in the microtubule organizing
233 center (MTOC) located in the vicinity of the nucleus [30]. To investigate the possibility that the perinuclear tau
234 accumulation in OptoTauKI cells after 12 hours of exposure to blue light is an aggresome, we performed
235 immunofluorescence staining for γ-tubulin in the MTOC, together with tau. The tau accumulation in the vicinity of the
236 nucleus observed immediately and 24 hours after the cessation of blue light was co-localized with γ-tubulin in MTOCs
237 (Figure. 4A, arrowheads). This result indicates that the MTOC is the site of tau accumulation after blue light
238 termination.
239 The process of transporting degenerated proteins along the microtube to the aggresome at MTOCs involves the
240 microtubule motor protein dynein and histone deacetylase 6 (HDAC6), which recruits denatured proteins to dynein
241 [31]. To investigate the possibility that the solid bright spots of tau that appeared in OptoTauKI cells after blue light
242 arrest were contained in aggresome and its precursors, we examined the co-localization of these aggresome marker
243 proteins with tau. Tau signal co-localized with HDAC6 and dynein in the near-nuclear bright spots (arrowheads) and
244 thick filaments (Figure. 4B and C, 0 h). At 24 h after the cessation of blue light, tau showed stronger co-localization
245 with HDAC6, or dynein, near the nucleus and in the cytoplasm. These results suggest that tau proteins are recruited to
246 aggresome-associated proteins and ultimately accumulated to the aggresome in OptoTauKI cells with 12 h continuous
247 blue light exposure.
248 Western blot experiments showed an increase in OptoTau of 150 kDa after 12 hours of illumination (Figure. 2D).
249 Immunostaining with RTM38 antibody also showed cells with increased tau after 12 hours of light exposure compared
250 to dark conditions (Figure. 4D, top). Interestingly, cells with increased tau upon light illumination had increased levels
251 of HDAC6 protein (Figure. 4D, bottom). This result suggests that the increase in tau levels and filamentous tau induced
252 by light stimulation may activate the formation of aggresomes.
253
254 **Insoluble tau aggregation induced by intermittent blue light illumination**
255 Continuous blue light irradiation for 12 hours induced tau translocation to the aggresome, where denatured proteins
256 accumulated but did not form stable aggregates, as seen in AD and other tauopathy. We next searched for conditions
257 that would induce stable tau aggregation in OptoTauKI cells. To increase the probability of tau molecules interacting in
258 an optimal position, we expected repeated cluster formation and dissociation of OptoTau would be effective. Taking
259 advantage of the 23.1 min half-life for dissociation of the CRY2Olig cluster [21], we designed an illumination cycle in

260 which a 30-min blue light exposure is followed by a 30-min dark period during which the CRY2Olig interactions are
261 lost (Figure 5A). OptoTauKI cells express the OptoTau protein stably, allowing for prolonged blue light illumination,
262 which was impossible in transfected cells in previous studies. Therefore, we performed a 24-hour illumination sequence
263 consisting of a 16-hour dark period followed by eight 30-minute dark/30-minute blue light cycles (repeated
264 illumination), which was continued for 6 to 8 days (Figure. 5A). The stability of the tau aggregation-like structures
265 induced by blue light was evaluated based on whether they remained 16 hours after the illumination was terminated.
266 Total tau labeled with RTM38 antibody showed a thick linear filament structure immediately after repeated illumination
267 for 6 and 8 days (Figure. 5B, RTM38). This filament structure was not seen in OptoKI cells with a 6-day illumination
268 cycle plus 16 hours of darkness but remained in cells with an 8-day illumination cycle plus 16 hours of darkness. The
269 MC1 antibody is an antibody that recognizes the initial conformation of pathological tau [32] [33]. MC1 antibody also
270 recognized the filament-like conformation immediately after the termination of repeated illumination and after 16 hours
271 of illumination cycle for 8 days (Figure. 5B, MC1), as did the RTM38 antibody. The percentage of cells with bright
272 solid spots showing stable tau aggregation 16 hours after termination of repeated illumination was significantly higher
273 after 8 days of illumination than after 6 days (Figure. 5C).
274 Taking advantage of that methanol fixation had the effect of removing soluble tau in the cytoplasm [26], we
275 examined whether repeated illumination to OptoTauKI cells results in the formation the insoluble tau. Methanol-fixed
276 cells immediately after 6 days of repeated irradiation showed RTM38-positive aggregation in the cytoplasm, but this
277 aggregation disappeared 16 hours later (Fig. 5D, Top). Immediately after 8 days of repeated illumination, the amount of
278 insoluble tau remaining after methanol fixation was increased compared to that after 6 days of illumination and was
279 detected as thick filament structures (Fig. 5D, 8 days). This filament-like tau remained as a methanol-insoluble structure
280 after 16 hours (Fig. 5D, 8 days+16 h). The results indicate that repeated blue light exposure and dark incubation over 8
281 days can produce insoluble tau aggregation.
282
283 **Acceleration of insoluble tau aggregation formation by short light-dark cycles**
284 Finally, we examined whether the temporal pattern of blue light/dark cycle repetitions affected the time to the induction
285 of insoluble tau aggregation. Here, 25 min dark/5 min blue light illumination cycles were repeated 48 times (Figure
286 6A). The total required time was 24 hours, with a total illumination time of 4 hours. A 25 min dark/5 min blue light
287 cycle for 24 h formed thick tau filaments as detected by RTM38 and MC1 antibodies (Figure 6, top). MC1-positive tau
288 filaments remained after 16 hours of dark incubation after the illumination cycle (Figure 6B, bottom). The insolubility

289 of filamentous tau in OptoTauKI cells immediately after the end of the cycle and after 16 hours of dark incubation after
290 the cycle was also supported by immunofluorescent staining after methanol fixation (Figure 6C). These results indicate
291 that insoluble tau could be induced in only 24 hours by repeating the 25 min dark/5 min blue light exposure cycle. The
292 same 48 cycles of light illumination did not induce stable tau aggregation when 8 set cycles of 30 min dark / 30 min
293 blue light were repeated for 6 days; despite the longer duration of each illumination (30 min vs. 5 min), total
294 illumination time (24 h vs. 4 h), and total time required (6 days vs 24 hours) (Figure 5). Furthermore, fibrous tau
295 aggregation was hardly formed by 144 cycles of 1 min blue light/9 min dark illumination, despite the high number of
296 cycles (data not shown). The results indicate that the temporal pattern, including the duration of one illumination,
297 interval time, and number of repetitions, must be set appropriately to introduce insoluble aggregation with OptoTau.
298 Interestingly, insoluble tau aggregates induced by the 5 min light/25 min dark cycle were less frequently located
299 near the nucleus where aggresomes were formed (Figure 4). In OptoTauKI cells illuminated continuously for 12 h, by
300 which accumulation of tau in the aggresome was observed, an average of 69.64 ± 2.90% (n=9) of the tau aggregates
301 were located in the nuclear vicinity. On the other hand, in cells illuminated for 24 h with 5 min light/25 min dark cycles,
302 significantly less tau aggregation was found in the vicinity of the nucleus (34.54 ± 4.06% (n=6)) (Figure 6D, $p<0.001$,
303 student's t-test). This result suggests that the insoluble tau induced by the 5 min blue light/25 min dark cycle escaped
304 translocation to aggresomes.
305
306 **Discussion**
307 In the present study, we generated cells knocking in OptoTau, an optogenetic tool based on the CRY2Olig module,
308 and established a technique to manipulate tau aggregation with blue light. We found light illumination conditions that
309 specifically induce tau accumulation in aggresomes or insoluble tau aggregation.
310
311 Recently, a series of studies have reported that transient overexpression of chimeric proteins combining tau with
312 CRY2 or its derivative CRY2Olig, i.e., families of OptoTau, results in the blue light-dependent formation of LLPS
313 droplets and tau oligomers [23] [24] [25]. In the present study, we manipulated tau by blue light in OptoTauKI cells, in
314 which OptoTau was inserted into the genome by genome editing. In dividing cells, the transfected plasmid is diluted by
315 cell division, and the expression level of the product is reduced. Here, using a cell line that stably expresses OptoTau
316 enabled us to validate the blue light illumination protocol over several days while maintaining OptoTau expression.
317 When SH SY5Y and HeLa cells overexpressing CRY2WT-mCherry-Tau, a protein fusing CRY2 and human wild-

type tau in a previous study, were exposed to blue light, tau condensate formed along microtubules within 50 seconds [23]. Our result that tau formed filament structures colocalizing with microtubules in OptoTauKI cells exposed to blue light for 12 hours is consistent with this report. On the other hand, exposure to blue light for 3 min to primary cortical culture neurons overexpressing "Tau::CRY2", which is CRY2Olig fused to the C-terminus of human wild-type tau, induced droplets and oligomers of tau [24]. In Neuro2a cells overexpressing our OptoTau, consisting of CRY2Olig-Snap-human Tau with P301L, such a droplet of tau, which is considered to be an LLPS droplet, was induced by 24 hour- blue light illumination in the presence of microtubule depolymerizing agent nocodazole [25]. However, no droplet-like structures were induced in OptoTauKI cells by any light illumination protocols in the present study. The differences in the morphology of the OptoTau complex induced by blue light may depend on multiple parameters, including the expression levels of OptoTau, endogenous tau in the cells, blue light exposure time, exposure intensity, cell type, and microtubule integrity.

Some filamentous tau induced by 12 hours of blue light illumination on OptoTauKI accumulated in MTOCs stained with γ-tubulin and co-localized with HDAC6 and dynein, both component proteins of aggresomes. OptoTau accumulation in aggresomes was also observed in Neuro2a cells overexpressing OptoTau [25]. The result that HDAC6 amount is increased in cells with increased tau content implies that tau degradation is triggered by selective autophagy. In this study, we did not confirm the up-regulation of tau ubiquitination, which is a signal for transport to aggresome. It also remains to be verified whether aggresome activity is increased after light stimulation, leading to degradation of OptoTau and endogenous Tau. Previous studies have shown that phosphorylated tau and tau oligomers are increased in the hippocampus of mice in which the aggresomal protein p62 is knocked out [34]. Optogenetically accumulated OptoTau co-localizes with endogenous p62 [25]. The role of p62 in light-induced aggresome formation and tau degradation needs to be further verified.

In this study, we found two illumination conditions induce methanol-insoluble tau aggregation: one is to repeat a 24-hour illumination sequence consisting of a 16-hour dark period followed by eight 30 min dark/30 min blue light cycles for 8 days, and another is repeating 25 min dark/5 min blue light cycles for 24 hours. This aggregation did not disappear even 16 hours after the termination of light illumination. Therefore, these tau aggregates are interpreted as a stable residual structure. Initial conformational changes in pathological tau labeled by the MC1 antibody were detected even before stable aggregation was generated but only remained when methanol-insoluble tau aggregation was present. In a previous study, sarcosyl-insoluble tau aggregation could be induced optogenetically by OptoTau with truncated N-

347 terminal of tau. Still, OptoTau with full-length tau did not induce insoluble tau aggregation [25]. Since the N-terminal
348 of tau inhibits polymerization of full-length tau [35], it is likely that OptoTau lacking its N terminal is more likely to
349 produce aggregation seed. The present study indicates that even full-length tau could be transformed into stable
350 aggregation by light illumination with repeated On/Off cycles. Opto-α-synuclein, α-synuclein fused with CRY2Olig,
351 was also induced to form stable aggregates in human iPS cell-derived neurons by repeated stimulation at 0.17 Hz.
352 Repeated on/off stimulation and periods of no light exposure are effective means of avoiding phototoxicity. In addition,
353 it may be necessary to repeatedly stimulate the CRY2Olig module to induce stable aggregation. In particular, OptoTau
354 is a microtubule-binding protein that can be trapped in microtubules, making it difficult to interact with each other at
355 optimal positions. The frequent concentration of OptoTau by blue light followed by dissociation during the dark period
356 may increase the possibility of interaction between tau molecules at appropriate positions. Indeed, by accelerating the
357 cycles of light illumination, stable aggregation could be induced in a shorter period (8 days to 24 hours), even though
358 the total time of blue light illumination was shorter (24 hours to 4 hours). This result suggests that tau aggregation can
359 be induced more efficiently when CRY2Olig binding/dissociation is repeated rapidly. This study only demonstrated two
360 conditions under which stable induction of tau aggregation is possible, and the optimal aggregation induction system
361 should be further explored.
362
363 In this study, we showed that OptoTau could induce opposing behaviors such as stable tau aggregation and
364 aggresome formations, i.e., proteolysis and protein aggregation, depending on the pattern of light stimulation. OptoTau
365 presents a new experimental possibility for future introduction into the mouse brain, where the assembly state of tau can
366 be manipulated with light at the intended timing in specific cells at the targeted brain region. This optogenetic tool
367 could also help to validate the existence of "singularity cells," i.e., a small number of rare cells that cause significant
368 changes throughout the system [18]. In Alzheimer's disease, the neurons that first form tau aggregates in LCs and ECs
369 can be assumed to be "singularity cells" [20]. If OptoTau can specifically induce tau aggregation only in LCs and ECs,
370 it will be possible to verify whether they can be "singularity cells" that spread tau pathology to the cortex.
371 Some issues need to be resolved before OptoTau can be used as a model for tauopathies in the future. One is the
372 isoform of tau. The tau isoform with the 31 amino acid repeats encoded by exon 10 is called the 4R isoform, and the
373 isoform without the repeats is called the 3R. The tau aggregates of AD and CTE contain 3R and 4R tau, while Pick's
374 disease is composed of only 3R tau, and CBD and PSP are composed of only 4R tau. The molecular structure of the
375 filaments within tau aggregates differs in each tauopathic disease [10]. The molecular structure of the tau aggregation

core is the determinant of the tau aggregate properties (including the ratio of 3R tau to 4R tau) specific to tauopathies [36]. Current OptoTau includes only 4R-type tau. In the future, it will be necessary to develop 3R-type OptoTau to create optogenetic models specific to AD, CTE, and Pick's disease. The 3R to 4R tau expression ratio in OptoTau-induced cells should be controlled. In addition, photogenetically inducing aggregation nuclei specific to each tauopathy will be a significant challenge.

Conclusion

This study used the optogenetic tool OptoTau, based on the CRY2Olig module, to induce tau aggregation in cells. Specific light exposure conditions introduced aggresome and insoluble aggregation in OptoTauKI cells. The present results will provide a new technological basis for creating a singular point of tau aggregation at a targeted time in targeted cells.

Conflict of Interest

The authors have no conflict of interest related to this publication.

Author Contributions

SS, TU, NK, BX, AH, and YS performed the experiment. SY, AT, HY, GM, and HB were involved in the design and supervision of this work. SS, TU, NK, BX, AH, and HB processed the experimental data, performed the analysis, drafted the manuscript, and designed the figures. All authors discussed the results and commented on the manuscript.

Data Availability

The evidence data generated and/or analyzed during the current study are available from the corresponding author upon reasonable request.

Acknowledgments

The authors thank Prof. Peter Davies (Albert Einstein College of Medicine) for providing the MC1 antibody, Dr Sumiyo Mimura (AS ONE Corporation) for technical support of single cell cloning, and Dr. Naruhiko Sahara (National Institutes for Quantum Science and Technology) for insightful discussion. This research was funded by Grant-in-Aid for Scientific Research on Innovative Areas "Singularity Biology" (JP18H05410 to HY, JP18H05414 to HB) from the

Ministry of Education, Culture, Sports, Science and Technology, Japan, JSPS Grants-in-Aid for Scientific Research JP20K06896, JP23K05993 to YS, JP21H02450, 23K18116 to HB. and medical research continuous grants from Takeda Science Foundation to HB. DeepL, ChatGPT 3.5, and Grammarly supported the English editing of this article.

References

[1] Gotz, J., Halliday, G., Nisbet, R.M. Molecular pathogenesis of the tauopathies. Annu Rev Pathol 14, 239-261 (2019). https://doi.org/10.1146/annurev-pathmechdis-012418-012936

[2] Alquezar, C., Arya, S., Kao, A.W. Tau post-translational modifications: Dynamic transformers of tau function, degradation, and aggregation. Front Neurol 11, 595532 (2020). https://doi.org/10.3389/fneur.2020.595532

[3] Braak, H., Del Tredici, K. The pathological process underlying alzheimer's disease in individuals under thirty. Acta Neuropathol 121, 171-181 (2011). https://doi.org/10.1007/s00401-010-0789-4

[4] Braak, H., Thal, D.R., Ghebremedhin, E., Del Tredici, K. Stages of the pathologic process in alzheimer disease: Age categories from 1 to 100 years. J Neuropathol Exp Neurol 70, 960-969 (2011). https://doi.org/10.1097/NEN.0b013e318232a379

[5] Ossenkoppele, R., Schonhaut, D.R., Schöll, M., Lockhart, S.N., Ayakta, N., Baker, S.L., et al. Tau pet patterns mirror clinical and neuroanatomical variability in alzheimer's disease. Brain 139, 1551-1567 (2016). https://doi.org/10.1093/brain/aww027

[6] Cho, H., Choi, J.Y., Hwang, M.S., Kim, Y.J., Lee, H.M., Lee, H.S., et al. In vivo cortical spreading pattern of tau and amyloid in the alzheimer disease spectrum. Annals of Neurology 80, 247-258 (2016). https://doi.org/https://doi.org/10.1002/ana.24711

[7] Allen, B., Ingram, E., Takao, M., Smith, M.J., Jakes, R., Virdee, K., et al. Abundant tau filaments and nonapoptotic neurodegeneration in transgenic mice expressing human p301s tau protein. J Neurosci 22, 9340-9351 (2002). https://doi.org/10.1523/jneurosci.22-21-09340.2002

[8] Santacruz, K., Lewis, J., Spires, T., Paulson, J., Kotilinek, L., Ingelsson, M., et al. Tau suppression in a neurodegenerative mouse model improves memory function. Science 309, 476-481 (2005). https://doi.org/10.1126/science.1113694

[9] Yoshiyama, Y., Higuchi, M., Zhang, B., Huang, S.M., Iwata, N., Saido, T.C., et al. Synapse loss and microglial activation precede tangles in a p301s tauopathy mouse model. Neuron 53, 337-351 (2007). https://doi.org/10.1016/j.neuron.2007.01.010

[10] Sahara, N., Yanai, R. Limitations of human tau-expressing mouse models and novel approaches of mouse modeling for tauopathy. Front Neurosci 17, 1149761 (2023). https://doi.org/10.3389/fnins.2023.1149761

[11] Iba, M., Guo, J.L., McBride, J.D., Zhang, B., Trojanowski, J.Q., Lee, V.M. Synthetic tau fibrils mediate transmission of neurofibrillary tangles in a transgenic mouse model of alzheimer's-like tauopathy. J Neurosci 33, 1024-1037 (2013). https://doi.org/10.1523/jneurosci.2642-12.2013

[12] Clavaguera, F., Akatsu, H., Fraser, G., Crowther, R.A., Frank, S., Hench, J., et al. Brain homogenates from human tauopathies induce tau inclusions in mouse brain. Proc Natl Acad Sci U S A 110, 9535-9540 (2013). https://doi.org/10.1073/pnas.1301175110

[13] Bell, B.J., Malvankar, M.M., Tallon, C., Slusher, B.S. Sowing the seeds of discovery: Tau-propagation models of alzheimer's disease. ACS Chem Neurosci 11, 3499-3509 (2020). https://doi.org/10.1021/acschemneuro.0c00531

[14] Narasimhan, S., Guo, J.L., Changolkar, L., Stieber, A., McBride, J.D., Silva, L.V., et al. Pathological tau strains from human brains recapitulate the diversity of tauopathies in nontransgenic mouse brain. J Neurosci 37, 11406-11423 (2017). https://doi.org/10.1523/JNEUROSCI.1230-17.2017

[15] Vogels, T., Leuzy, A., Cicognola, C., Ashton, N.J., Smolek, T., Novak, M., et al. Propagation of tau pathology: Integrating insights from postmortem and in vivo studies. Biol Psychiatry 87, 808-818 (2020). https://doi.org/10.1016/j.biopsych.2019.09.019

[16] Calafate, S., Buist, A., Miskiewicz, K., Vijayan, V., Daneels, G., de Strooper, B., et al. Synaptic contacts enhance cell-to-cell tau pathology propagation. Cell Reports 11, 1176-1183 (2015). https://doi.org/https://doi.org/10.1016/j.celrep.2015.04.043

[17] Pérez, M., Avila, J., Hernández, F. Propagation of tau via extracellular vesicles. Frontiers in Neuroscience 13 (2019). https://doi.org/10.3389/fnins.2019.00698

[18] Nagai, T. Editorial: Singularity biology and beyond. Biophysics and Physicobiology advpub (2024). https://doi.org/10.2142/biophysico.bppb-v21.s013

[19] Ichimura, T., Kakizuka, T., Sato, Y., Fujioka, Y., Ohba, Y., Horikawa, K., et al. Strength in numbers: Unleashing the potential of trans-scale scope amateras for massive cell quantification. Biophysics and Physicobiology advpub (2024). https://doi.org/10.2142/biophysico.bppb-v21.s017

[20] Bannai, H., Takashima, A., Soeda, Y., Yoshimura, H., Matsumoto, G., Sahara, N., et al. Research on the molecular mechanism of singularity phenomenon in neurological disorders. Biophysics and Physicobiology

advpub (2024). https://doi.org/10.2142/biophysico.bppb-v21.s008

[21] Taslimi, A., Vrana, J.D., Chen, D., Borinskaya, S., Mayer, B.J., Kennedy, M.J., et al. An optimized optogenetic clustering tool for probing protein interaction and function. Nat Commun 5, 4925 (2014). https://doi.org/10.1038/ncomms5925

[22] Tiwari, P., Tolwinski, N.S. Using optogenetics to model cellular effects of alzheimer's disease. Int J Mol Sci 24 (2023). https://doi.org/10.3390/ijms24054300

[23] Zhang, X., Vigers, M., McCarty, J., Rauch, J.N., Fredrickson, G.H., Wilson, M.Z., et al. The proline-rich domain promotes tau liquid-liquid phase separation in cells. J Cell Biol 219 (2020). https://doi.org/10.1083/jcb.202006054

[24] Jiang, L., Lin, W., Zhang, C., Ash, P.E.A., Verma, M., Kwan, J., et al. Interaction of tau with hnrnpa2b1 and n(6)-methyladenosine rna mediates the progression of tauopathy. Mol Cell 81, 4209-4227 e4212 (2021). https://doi.org/10.1016/j.molcel.2021.07.038

[25] Soeda, Y., Yoshimura, H., Bannai, H., Koike, R., Takashima, A. Intracellular tau fragment droplets serve as seeds for tau fibrils. bioRxiv, 2023.2009.2010.557018 (2023). https://doi.org/10.1101/2023.09.10.557018

[26] Guo, J.L., Narasimhan, S., Changolkar, L., He, Z., Stieber, A., Zhang, B., et al. Unique pathological tau conformers from alzheimer's brains transmit tau pathology in nontransgenic mice. J Exp Med 213, 2635-2654 (2016). https://doi.org/10.1084/jem.20160833

[27] Gyparaki, M.T., Arab, A., Sorokina, E.M., Santiago-Ruiz, A.N., Bohrer, C.H., Xiao, J., et al. Tau forms oligomeric complexes on microtubules that are distinct from tau aggregates. Proc Natl Acad Sci U S A 118 (2021). https://doi.org/10.1073/pnas.2021461118

[28] Guthrie, C.R., Kraemer, B.C. Proteasome inhibition drives hdac6-dependent recruitment of tau to aggresomes. J Mol Neurosci 45, 32-41 (2011). https://doi.org/10.1007/s12031-011-9502-x

[29] Santa-Maria, I., Varghese, M., Ksiezak-Reding, H., Dzhun, A., Wang, J., Pasinetti, G.M. Paired helical filaments from alzheimer disease brain induce intracellular accumulation of tau protein in aggresomes. J Biol Chem 287, 20522-20533 (2012). https://doi.org/10.1074/jbc.M111.323279

[30] Kopito, R.R. Aggresomes, inclusion bodies and protein aggregation. Trends Cell Biol 10, 524-530 (2000). https://doi.org/10.1016/s0962-8924(00)01852-3

[31] Kawaguchi, Y., Kovacs, J.J., McLaurin, A., Vance, J.M., Ito, A., Yao, T.-P. The deacetylase hdac6 regulates aggresome formation and cell viability in response to misfolded protein stress. Cell 115, 727-738 (2003). https://doi.org/https://doi.org/10.1016/S0092-8674(03)00939-5

[32] Jicha, G.A., Bowser, R., Kazam, I.G., Davies, P. Alz-50 and mc-1, a new monoclonal antibody raised to paired helical filaments, recognize conformational epitopes on recombinant tau. J Neurosci Res 48, 128-132 (1997). https://doi.org/10.1002/(sici)1097-4547(19970415)48:2<128::aid-jnr5>3.0.co;2-e

[33] Jicha, G.A., Lane, E., Vincent, I., Otvos, L., Jr., Hoffmann, R., Davies, P. A conformation- and phosphorylation-dependent antibody recognizing the paired helical filaments of alzheimer's disease. J Neurochem 69, 2087-2095 (1997). https://doi.org/10.1046/j.1471-4159.1997.69052087.x

[34] Ono, M., Komatsu, M., Ji, B., Takado, Y., Shimojo, M., Minamihisamatsu, T., et al. Central role for p62/sqstm1 in the elimination of toxic tau species in a mouse model of tauopathy. Aging Cell 21, e13615 (2022). https://doi.org/10.1111/acel.13615

[35] Horowitz, P.M., LaPointe, N., Guillozet-Bongaarts, A.L., Berry, R.W., Binder, L.I. N-terminal fragments of tau inhibit full-length tau polymerization in vitro. Biochemistry 45, 12859-12866 (2006). https://doi.org/10.1021/bi061325g

[36] Hosokawa, M., Masuda-Suzukake, M., Shitara, H., Shimozawa, A., Suzuki, G., Kondo, H., et al. Development of a novel tau propagation mouse model endogenously expressing 3 and 4 repeat tau isoforms. Brain 145, 349-361 (2021). https://doi.org/10.1093/brain/awab289

511 **Figure Legends**

512

513 **Figure 1: Neuro2a knock-in Neuro2a cells**

514 (A) Top: design of OptoTau, which consists of CRY2Olig, SNAP-tag, and human2N4R tau with P301L mutation/
515 Bottom: conceptual diagram of OptoTau knock-in to mouse ROSA26 locus using CRISPR/Cas9 system. The donor
516 vector contains OptoTau expressed under the CMV promoter and GFP and Puromycin (Puro) sequences for screening.

517 (B) Live cell imaging of GFP and SNAP647 fluorescence in Neuro2A cells (WT) and OptoTau knock-in Neuro2a cells
518 (OptoTauKI). The SNAP647 signal reflects the localization of OptoTau. Transmission images (Trans) were taken
519 from the same field of view. Bar: 10 μm.

520 (C) Confocal images of GFP and SNAP647 fluorescence in Neuro2A cells (WT) and Neuro2a cells knocking in OptoTau
521 knock-in (WT). Cells were fixed with 4% PFA. Bar: 10 μm.

522

523 **Figure 2: Effect of 12 hours of blue light illumination on Tau in OptoTau knock-in cells.**

524 (A) Subcellular localization of GFP (left), OptoTau (middle, SNAP647), and total Tau shown by immunofluorescence
525 staining with RTM38 antibody in OptoTau Knock-in cells. Top: cells kept in the dark condition (Dark, D); bottom:
526 cells fixed immediately after 12 h blue light (12 h blue light, L). Scale bar: 10 μm.

527 (B) Immunofluorescence staining images of microtubules (middle, α-tubulin) and total Tau (left, RTM38) in OptoTauKI
528 cells immediately after 12 hours of blue light illumination. The right panel shows the merge of these signals (a-
529 tubulin: green, total Tau: magenta). The scale bar represents 10 μm.

530 (C) Western blotting analysis of Tau using RTM38 antibody in Neuro2a cells (WT) and OptoTauKI cells (OptoTauKI).
531 D: cells under dark; L: cells illuminated with blue light for 12 h. 151 kDa and 115 kDa bands were detected. β-actin
532 was used as a loading control.

533 (D) Quantification of 115 kDa (left) and 151 kDa (right) tau. The ratio of β-actin-normalized tau band intensity to that
534 of Neuro2a cells (WT) was defined as relative Tau intensity. D: under dark, L: 12 h blue light exposure. NS: $p>0.1$,
535 *: $p<0.05$, Mann-Whitney U-test.

536

537 **Figure 3: Localization change of Tau after cessation of blue light illumination**

538 (A) Schematic illustration of the experimental design. Top: Localization of total Tau in OptoTauKI cells cultured in the
539 dark after 12 h of blue light illumination was verified by immunofluorescence staining with the RTM38 antibody;

540 the arrowhead indicates the timing of cell fixation. Dark indicates cells cultured in the dark for 12 h.

541 (B) Immunofluorescence images of total tau and microtubules immediately (0 h), 24 h, 48 h, and 72 h after cessation of

542 blue light exposure. Top: RTM38 antibody, middle: α-tubulin antibody, bottom: Merge image. Yellow arrowheads

543 indicate large bright spots of Tau; arrows indicate fragmented bright spots of Tau. Scale bar: 10 μm.

544

545 **Figure 4: Co-localization of tau with aggresome proteins after cessation of blue light illumination.**

546 Multicolor immunofluorescence images of Tau and aggresomal proteins in OptoTauKI cells immediately (0 h) and 24 h

547 after stopping 12 h blue light illumination. Aggresomal proteins labeled were (A) γ-tubulin, (B) HDAC6, and (C)

548 Dynein. (D) Immunostaining of Tau (RTM38, top) and HDAC6 (bottom) under dark conditions (Dark) and

549 immediately after 12 h of blue light exposure (Blue light). rrowheads show strong bright spots of Tau. he scale Bar is 10

550 μm.

551

552 **Figure 5: Formation of insoluble tau aggregates by repeated blue light illumination.**

553 (A) Protocol for repeated blue light stimulation. OptoTauKI cells were cultured in darkness for 16 hours, followed by 8

554 cycles of 30 min darkness/30 min blue light illumination, repeated for N days. Arrows indicate the timing of fixation.

555 (B) Immunofluorescence staining using total tau antibody (RTM38) and tau conformation change recognition antibody

556 (MC1) in OptoTauKI cells after repeated blue light stimulation. Cells cultured in the dark for 6 days (6 days Dark),

557 cells fixed immediately after repeated blue light stimulation on day 6 (6 days), cells fixed at 16 hours after day 6

558 light stimulation (6 day+16 h), cells fixed immediately after repeated blue light stimulation on day 8 (8 days), cells

559 fixed at 16 hours after day 8 light stimulation (8 day+16 h). Bar: 10 μm.

560 (C) Percentage of cells with insoluble tau aggregation 16 h after repeated blue light exposure. The red lines indicate

561 median. 6 days+16 h: N=46 cells; 8 days+16 h: N=31 cells. ****: $p<0.0001$, Mann-Whitney U-Test.

562 (D) Visualization of intracellular insoluble Tau by methanol fixation at 6 days and 6 days+16 h (top), 8 days and 8

563 days+16 h (bottom), using RTM38 antibody. Scale bar is 10 μm.

564

565 Figure 6: Acceleration of insoluble tau aggregation formation by repeated blue light illumination.

566 (A) Protocol for repeated blue light stimulation. The cycle was repeated for 48 consecutive cycles (24 h), each cycle

567 consisting of 25 min of darkness and 5 min of blue light illumination and. Arrows indicate the timing of fixation.

568 (B) Immunofluorescence staining using total tau antibody (RTM38) and tau conformation change recognition antibody

(MC1) in OptoTauKI cells after repeated blue light stimulation. PFA fixation was performed immediately after the end of 48 cycles (48 cycles + 0 h) or 16 h after the end of 48 cycles (48 cycles + 16 h) in the blue light (Blue light) and dark condition (Dark) groups, respectively. Bar: 10 µm.

(C) Visualization of intracellular insoluble Tau by methanol fixation. Methanol fixation was performed immediately after the end of 48 cycles (48 cycles + 0 h) or 16 h after the end of 48 cycles (48 cycles + 16 h) in the blue light (Blue light) and dark condition (Dark) groups, respectively. Scale bar is 10 µm.

(D) Comparison of the percentage of cells with perinuclear insoluble Tau accumulation of the single 12 h blue light illumination (BL12 h x 1) and the 48 repetitions of 5 min off 25 min blue light illumination [(BL5m + DK25m) x 1]. Fixation was performed immediately after completion of the total blue light illumination program in both groups. The red lines indicate median. BL12 h x 1: N=9 coverslips; (BL5m + DK25m) x 1: N=6 coverslips. ***: $p<0.001$, Student's t-test.

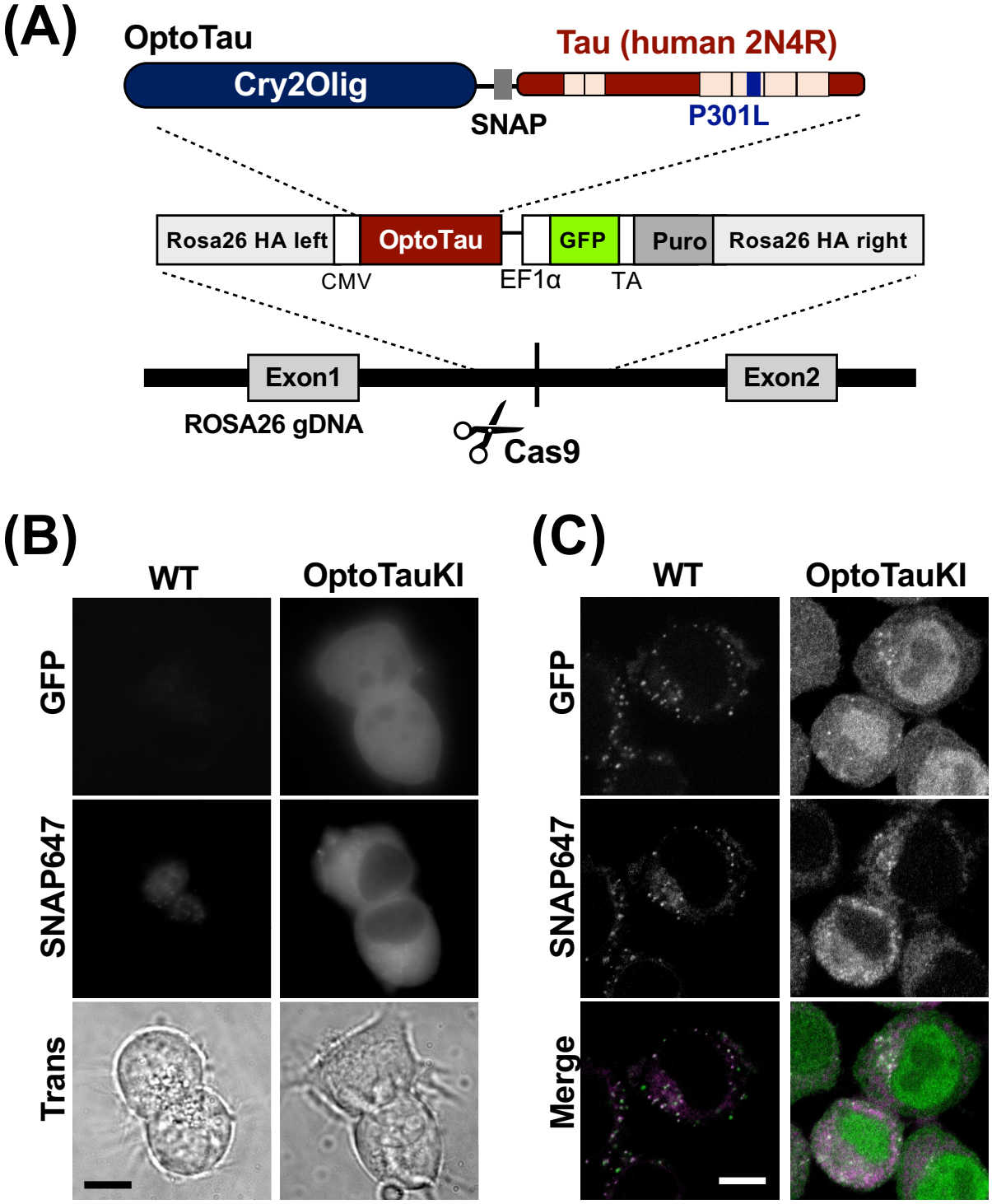
(A)
OptoTau
Cry2Olig
SNAP
Tau (human 2N4R)
P301L
Rosa26 HA left
OptoTau
GFP
Puro
Rosa26 HA right
CMV
EF1α
TA
Exon1
Exon2
ROSA26 gDNA
Cas9
(B)
WT
OptoTauKI
GFP
SNAP647
Trans
(C)
WT
OptoTauKI
GFP
SNAP647
Merge

Figure 1

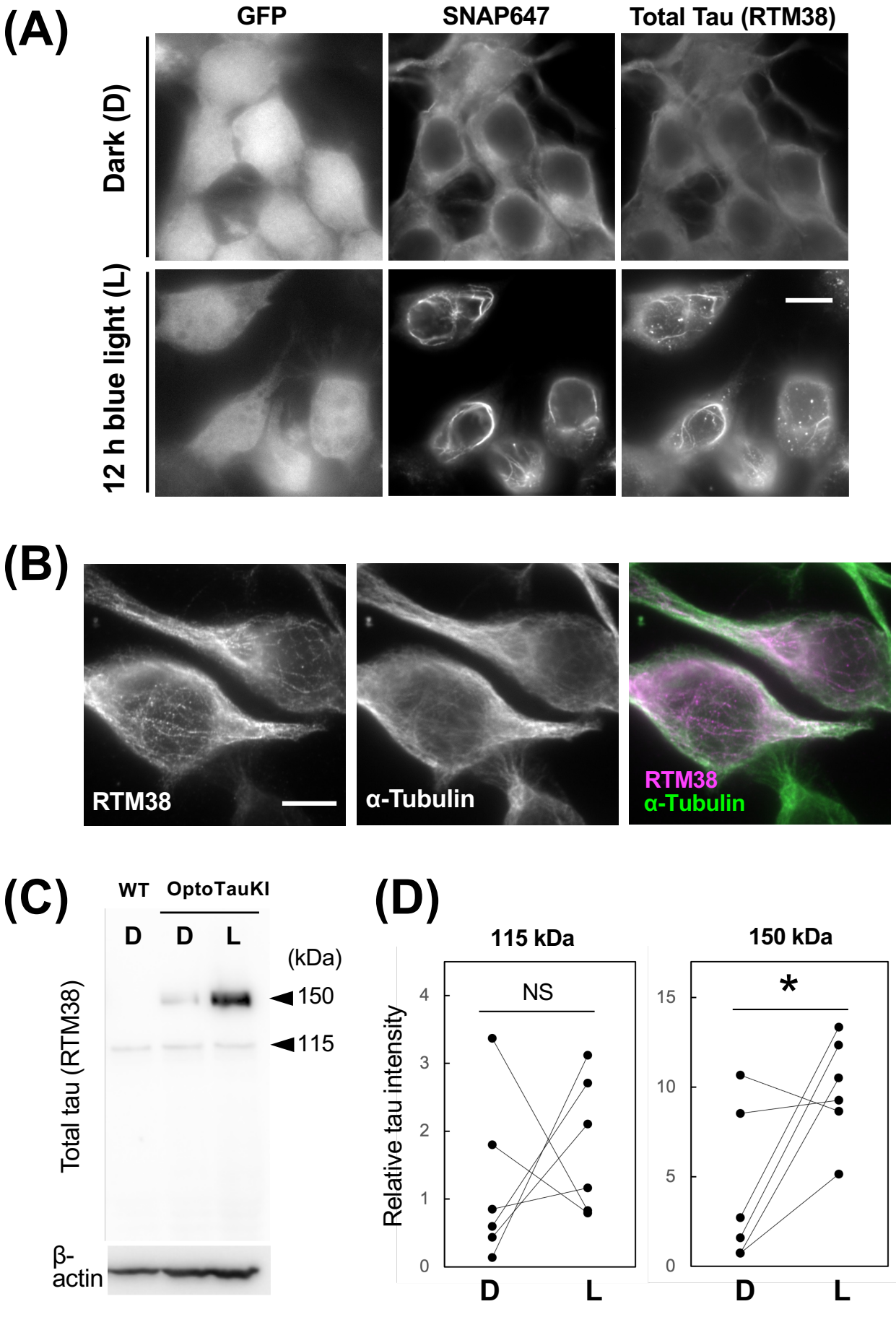
(A)
GFP
SNAP647
Total Tau (RTM38)
Dark (D)
12 h blue light (L)
(B)
RTM38
α-Tubulin
RTM38
α-Tubulin
(C)
WT
OptoTauKI
D
D
L
(kDa)
150
115
Total tau (RTM38)
β-actin
(D)
115 kDa
150 kDa
NS
*
Relative tau intensity
0
1
2
3
4
0
5
10
15
D
L
D
L

Figure 2

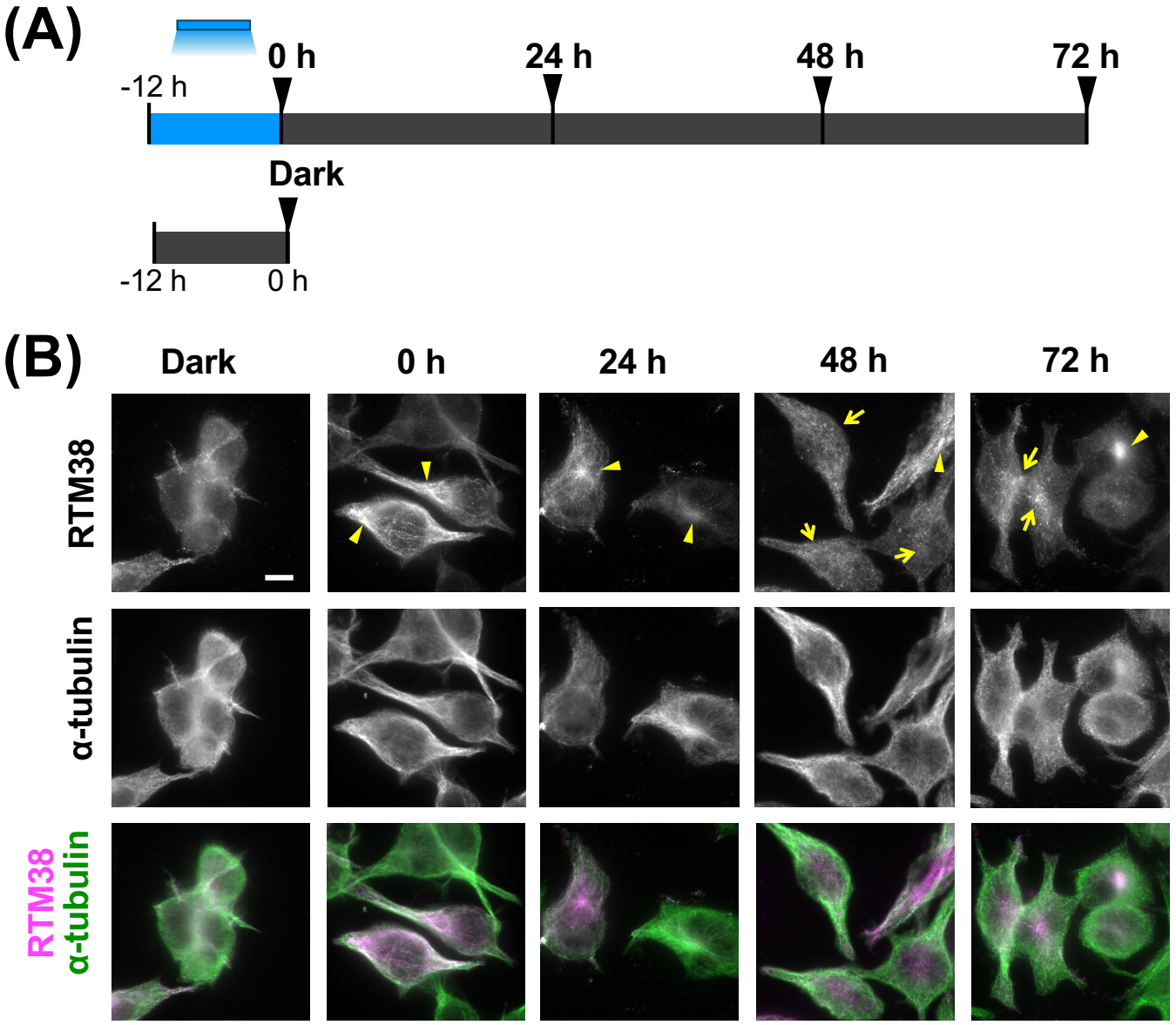
(A)
-12 h
0 h
24 h
48 h
72 h
Dark
-12 h
0 h
(B)
Dark
0 h
24 h
48 h
72 h
RTM38
α-tubulin
RTM38
α-tubulin

Figure 3

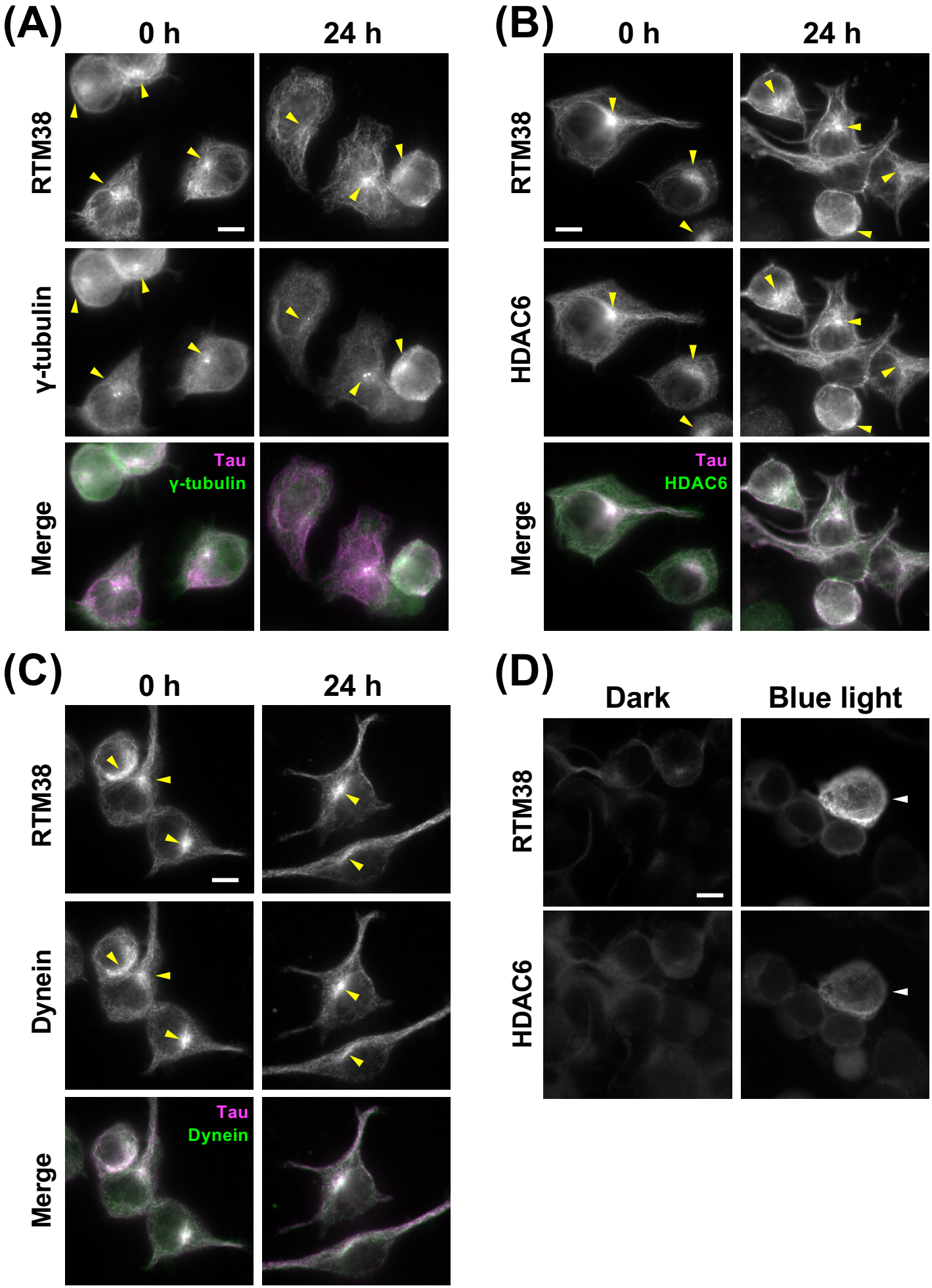
(A)
0 h
24 h
RTM38
γ-tubulin
Merge
Tau
γ-tubulin
(B)
0 h
24 h
RTM38
HDAC6
Merge
Tau
HDAC6
(C)
0 h
24 h
RTM38
Dynein
Merge
Tau
Dynein
(D)
Dark
Blue light
RTM38
HDAC6

Figure 4

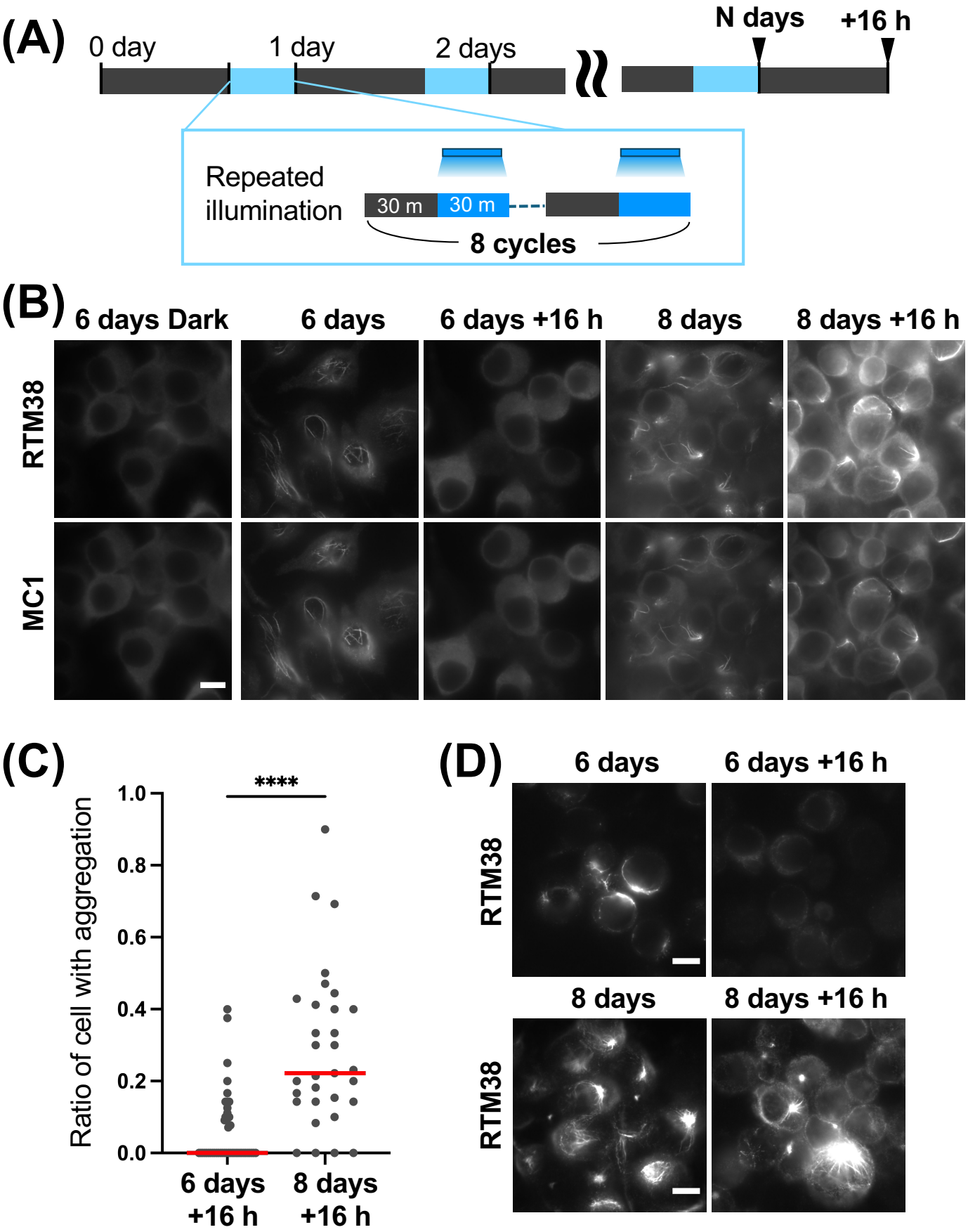
(A)
0 day
1 day
2 days
N days
+16 h
Repeated illumination
30 m
30 m
8 cycles
(B)
6 days Dark
6 days
6 days +16 h
8 days
8 days +16 h
RTM38
MC1
(C)
Ratio of cell with aggregation
1.0
0.8
0.6
0.4
0.2
0.0
****
6 days +16 h
8 days +16 h
(D)
6 days
6 days +16 h
RTM38
8 days
8 days +16 h
RTM38

Figure 5

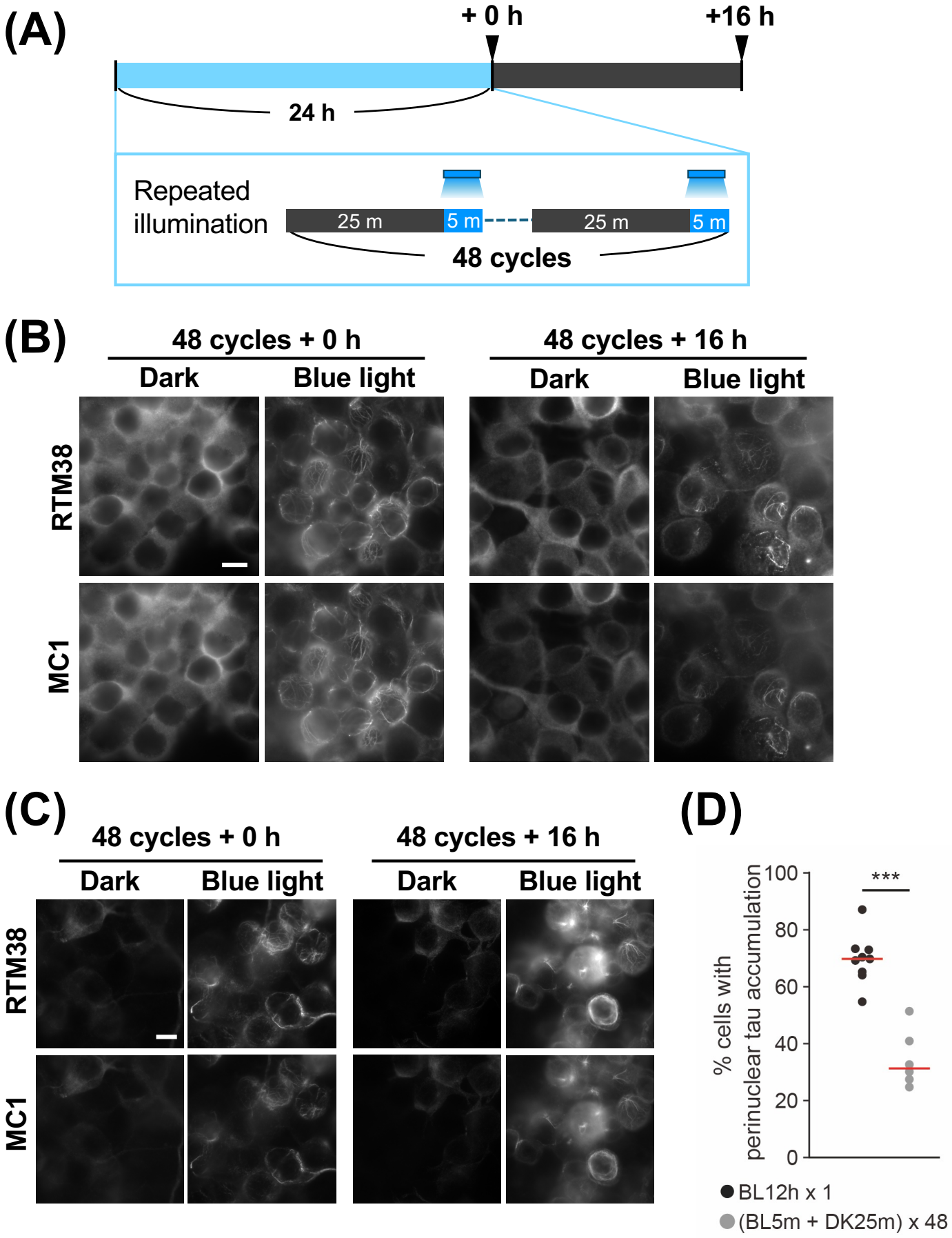
(A)
+ 0 h
+16 h
24 h
Repeated illumination
25 m
5 m
25 m
5 m
48 cycles
(B)
48 cycles + 0 h
48 cycles + 16 h
Dark
Blue light
Dark
Blue light
RTM38
MC1
(C)
48 cycles + 0 h
48 cycles + 16 h
Dark
Blue light
Dark
Blue light
RTM38
MC1
(D)
% cells with perinuclear tau accumulation
100
80
60
40
20
0
***
BL12h x 1
(BL5m + DK25m) x 48

Figure 6